J. Braz. Chem. Soc., Vol. 21, No. 9, 1718-1726, 2010.
Printed in Brazil - ©2010 Sociedade Brasileira de Química
0103 - 5053 $6.00+0.00

Revisiting the Origin of the Preferential π–π Stacking Conformation of the (+)-8-Phenylmenthyl Acrylate

Saulo L. Capim, Sidney R. Santana, Boaz G. de Oliveira, Gerd B. Rocha* and Mário L. A. A. Vasconcellos*

*Departamento de Química, Universidade Federal da Paraíba, Campus I,
58059-900 João Pessoa-PB, Brazil*

Neste artigo reportamos um estudo teórico objetivando revisitar a origem da conformação π–π *stacking* do (+)-acrilato de 8-fenilmentila (**2**) ser a preferencial. Para isso, calculamos geometrias de mínimo local, freqüências vibracionais, propriedades termoquímicas e deslocamentos químicos de RMN de ^{1}H para **2** e para o composto modelo acrilato de 3-fenilpropila (**3**) usando vários métodos *ab initio* e de DFT. Observamos que o funcional MPW1B95 foi o método mais apropriado em explicar os dados experimentais de RMN de ^{1}H nos quais mostram que a conformação *stacking* de **2** (**2***S*) é mais estável que a conformação *trans* (**2***T*) e a conformação *stacking* de **3** (**3***S*) é menos estável que a conformação *trans* (**3***T*). Após isso, detalhes geométricos e energéticos do complexo intermolecular benzeno...metilacrilato (**4**) também foram estudados usando o método MPW1B95. A partir dos nossos resultados percebemos que ambos os efeitos, estérico e de dispersão, desempenham papéis chave no equilíbrio conformacional de **2**.

In this paper we report a theoretical study aiming to revisit the origin of the preferential π–π stacking conformation of the (+)-8-phenylmentyl acrylate (**2**). For this, we have applied several DFT and *ab initio* methods to calculate local minimum geometries, vibrational frequencies, thermochemical properties and ^{1}H NMR chemical shifts for **2** and the model compound 3-phenylpropyl acrylate (**3**). We have observed that the MPW1B95 functional was the most suitable method to explain ^{1}H NMR experimental data which show the stacking conformation of **2** (**2***S*) is more stable that *trans* conformation (**2***T*) and the stacking conformation of **3** (**3***S*) is less stable that *trans* conformation (**3***T*). After that, geometrical and energetic features of the intermolecular complex benzene…methylacrylate (**4**) have also been studied using MPW1B95 method. From our results, we have noticed that both steric and dispersion effects play a key role in the conformational equilibrium of **2**.

Keywords: conformational analysis, intramolecular π–π *stacking* interactions, MPW1B95 functional, chiral auxiliaries, enantioselective synthesis

Introduction

Since 1975, when Corey and Ensley[1] used (+)-8-phenylmenthol (**1**) (Figure 1) for the preparation of the acrylate derivative (**2**) for enantioselective synthesis of prostaglandins, compound **1** has ranked among the most versatile chiral auxiliary in the toolbox of asymmetric organic synthesis, being especially useful for π-face-differentiation.[2] The presence of an aromatic nucleus is a salient feature common to many chiral auxiliaries, particularly those which provide the highest level of stereocontrol. The special stabilization in the stacking conformation (**2***S*) by π–π dispersion interaction between the aromatic and the acrylate groups has emerged as one of the most attractive explanations.[3] For example, Ulukanli *et al.*[4] described the aziridination of compound **2** in high diastereoselectivity using 3-acetoxyamino-2-ethylquinazolinone. According to the transition state proposed by Ulukanli *et al.,*[4] the reaction occurs selectively on the *si* face of the acrylate moiety of **2** due to hindrance of the aromatic benzene ring on the *re* face (see Scheme 1).

However, up to now there are some questions to be answered: is the attractive dispersion interaction between the phenyl group and the acrylate moiety in **2***S* (increasing its relative stability) the only effect which controls the preferential π–π stacking conformation of **2** (Figure 1)?

---

*e-mail: mlaav@quimica.ufpb.br, gbr@quimica.ufpb.br

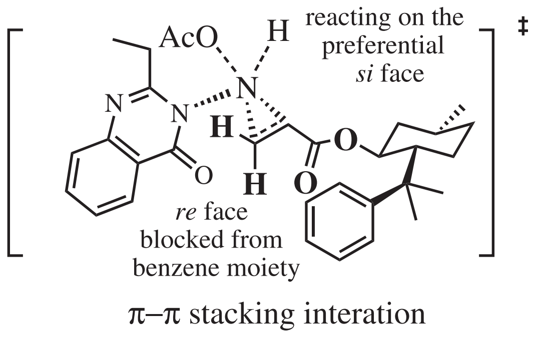

Scheme 1. Transition state of the aziridination of (+)-8-phenylmenthyl acrylate (**2**) using 3-acetoxyamino-2-ethylquinazolinone.

Could it be the steric repulsion effect, *e.g.* between one of the methyl groups and the acrylate moiety in **2***T*,[5] (increasing its relative energy) also an important effect to be considered? Or perhaps it is the case that both effects are controlling the preferential π–π stacking conformation of **2**? As far as we know, there are no theoretical studies involving density functional theory (DFT) and *ab initio* methodologies aiming to evaluate the actual origin of the relative stabilities of **2***S* and **2***T* conformations.

A survey of the recent chemical literature reveals an explosion of interest in the theoretical studies of non-covalent intermolecular interactions, specially the π–π stacking ones.[6] However, these kinds of studies for intramolecular π–π stacking interactions, using theoretical methods, are still very lacking.[6]

High-level quantum chemical calculations coupled with large basis sets covering large portions of correlation energy are required to describe accurately the non-covalent dispersion interactions.[7-9] For large structures or complexes, these high-level quantum chemical calculations cannot be carried out due to the high computational demand. For small or medium molecular structures we can apply second-order Møller-Plesset perturbation theory (MP2), which approximately accounts for uncoupled, two-body electron correlations. Unfortunately, some authors have detected that MP2 combined with an extended basis set tends to overestimate binding in non-covalent interactions.[10,11] On the other hand, DFT has been used as one of the most efficient theories to estimate non-covalent effects.[7-9,12,13] Recently, M. Swart *et al.*[14] have surprisingly shown that the LSDA functional was the most effective to evaluate π–π stacking interaction, compared with others DFT methods, including the KT1 and KT2. At the same time, Moa *et al.*[15] have performed DFT single-point calculations on the X-ray geometry of the quinone-hydroquinone (quinhydrone) intermolecular complex, and they were able to reproduce the experimental enthalpy when they used the method MPW1B95/6-311++G(2d,2p) with Cartesian *d* function for polarization atomic orbitals.

Then, in connection to our interests on developing new chiral auxiliaries,[16-20] synthesis[21] and conformational studies[22] of the new aromatic acrylate compounds to act as drugs,[23-25] we present in this paper a theoretical study involving DFT and *ab initio* methodologies aiming: (*i*) to discover which method is more suitable to estimate π–π stacking interactions between aromatic and acrylate moieties for medium-size systems and (*ii*) to evaluate if the intramolecular π–π stacking interactions really are the only effects that controls the conformation of (+)-8-phenylmenthyl acrylate (**2**).

Computational Details

First, we have used Hartree Fock (HF), MPW1B95,[26] M06,[27] M06-2X,[27] B97D[28] (this functional includes dispersion corrections) and MP2 in order to find the gas phase local minima of **2***S*, **2***T*, **3***S* and **3***T* (Figure 2). For this step, we have used the basis set 6-311++G(2d,2p) considering Cartesian *d* functions for polarization (6d opition in Gaussian input) for all calculations. All local minimum geometries were fully optimized without any symmetry constraints. After that, we have characterized each local minimum geometry by normal coordinate analysis at the corresponding theoretical level.

Next, the optimized geometries obtained from MPW1B95 were used on several single point energy calculations on MPWB1K,[26] MPW1B95,[26] M06,[27] M06-2X,[27] B97D,[28] LSDA,[29] B3LYP,[30,31] B3LYP-D,[32] B3PW91,[33] MPW1PW91,[34] HCTH,[35] PBE1PBE,[36.37] Hartree-Fock, second- and third-order Møller-Plesset perturbation theory (MP2 and MP3), Spin-component scaling MP2 (SCS-MP2)[38] and Spin-component scaling MP3 (SCS-MP3)[39] methodologies.

These calculations were carried out using GAUSSIAN 2003,[40] GAUSSIAN 2009[41] and ORCA (only for B3LYP-D).[42]

In order to verify the eficiency of MPW1B95 functional to predict the conformers for molecules **2** and **3**, we have performed some calculation of ^{1}H NMR chemical shifts using gauge invariant atomic orbital GIAO methodology[43] on the MPW1B95 local minimum geometries of all studied conformers, including solvent effects through PCM[44] methodology considering chloroform as solvent. ^{1}H NMR chemical shifts calculation for Tetramethyl silane, TMS, considered as the reference, were carried out using the same method, basis set and PCM conditions.

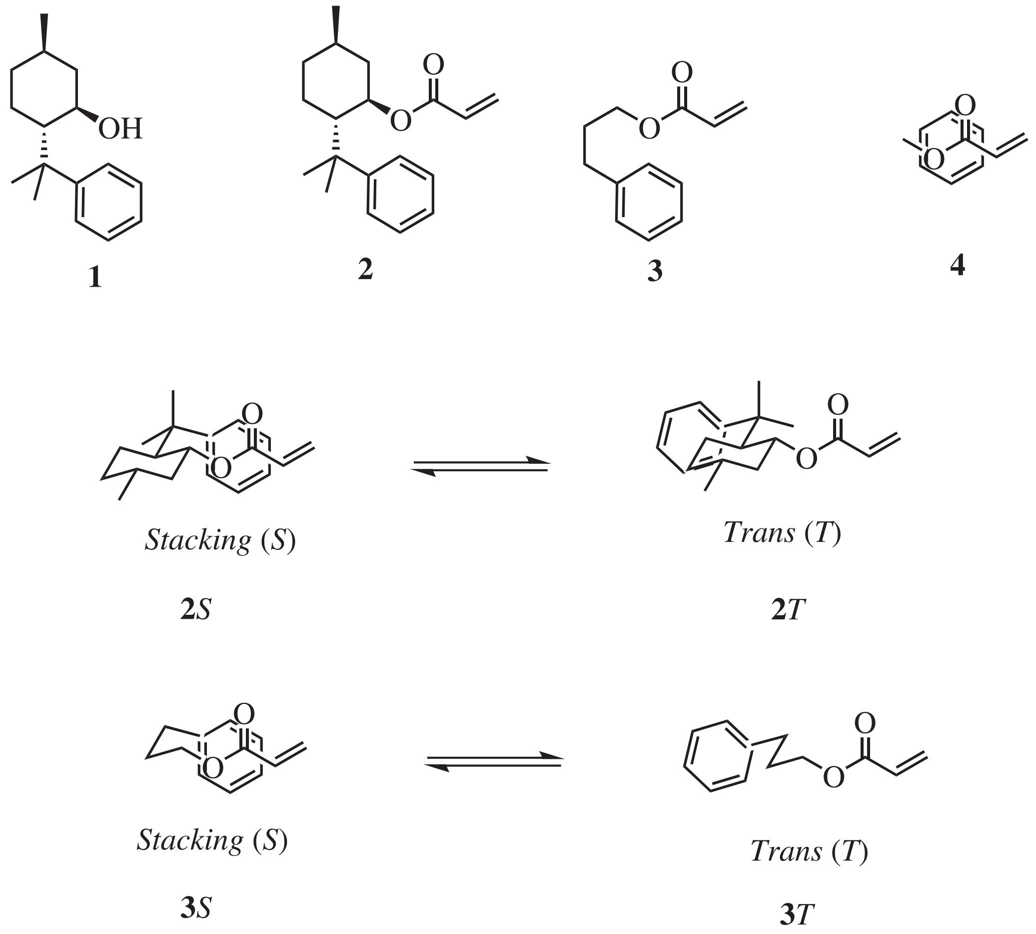

1 **2** **3** **4**

Stacking (*S*) **2***S*

Trans (*T*) **2***T*

Stacking (*S*) **3***S*

Trans (*T*) **3***T*

Figure 1. Structures for calculated conformations.

Finally, for the non-covalent complex **4**, we have performed calculations (geometry optimization and frequencies) using MPW1B95 and the same basis set with and without the counterpoise (CP) corrections for basis set superposition error (BSSE).[45,46]

Results and Discussion

First, we will qualitatively describe geometrical features for the considered conformations of compounds **2** and **3** (see Figure 2) in order to simplify our discussions.

For compound **2** we have two clear situations: (*i*) in the conformation **2***S* the phenyl group make π–π stacking interaction with the methyl acrylate group while one of the benzylic methyl group is located in *trans* position, (*ii*) in the conformation **2***T* we have the phenyl group in *trans* position while one of the benzylic methyl is located interacting with the methyl acrylate group.

For compound **3** the situation is almost the same. The difference between conformations **3S** and **3***T* is that in benzylic positions we now have hydrogen atoms, which present a smaller molecular volume.

It is important to notice that previous experimental data obtained by ^{1}H NMR spectra[1,47,48] (all spectra were obtained in deuterated chloroform and at room temperature) confirms that the **2***S* conformation is more stable than the **2***T* on (+)-8-phenylmentyl acrylate (**2**) and, the **3***T* conformation is more stable than **3***S* on 3-phenylpropyl acrylate (**3**).

In Figure 3 and table 1 we present the comparison between the ^{1}H NMR data for the hydrogen atoms H^1, H^2 and H^3 in methyl acrylate (**5**),[47] 3-phenylpropyl acrylate[48] (**3**) and (+)-8-phenylmenthyl acrylate (**2**).[1] From these experimental data it is possible to point out which conformation is more stable for compounds **2** and **3**.

We can note in table 1 that there is no significant shielding effect on H^1, H^2 and H^3 in **3** when compared with the corresponding hydrogen H^1, H^2 and H^3 in **5** ($\Delta\delta$ = 0.03 ppm for H^1; 0.01 for H^2 and 0.05 for H^3). These data confirm that the conformation **3***T* is more stable than **3***S* on this equilibrium. Note that in the conformation **3***S*, the hydrogen atoms H^1, H^2 and H^3 are positioned in the anisotropic shielding of the aromatic ring. So, if the conformation **3***S* was the most stable, we would expect

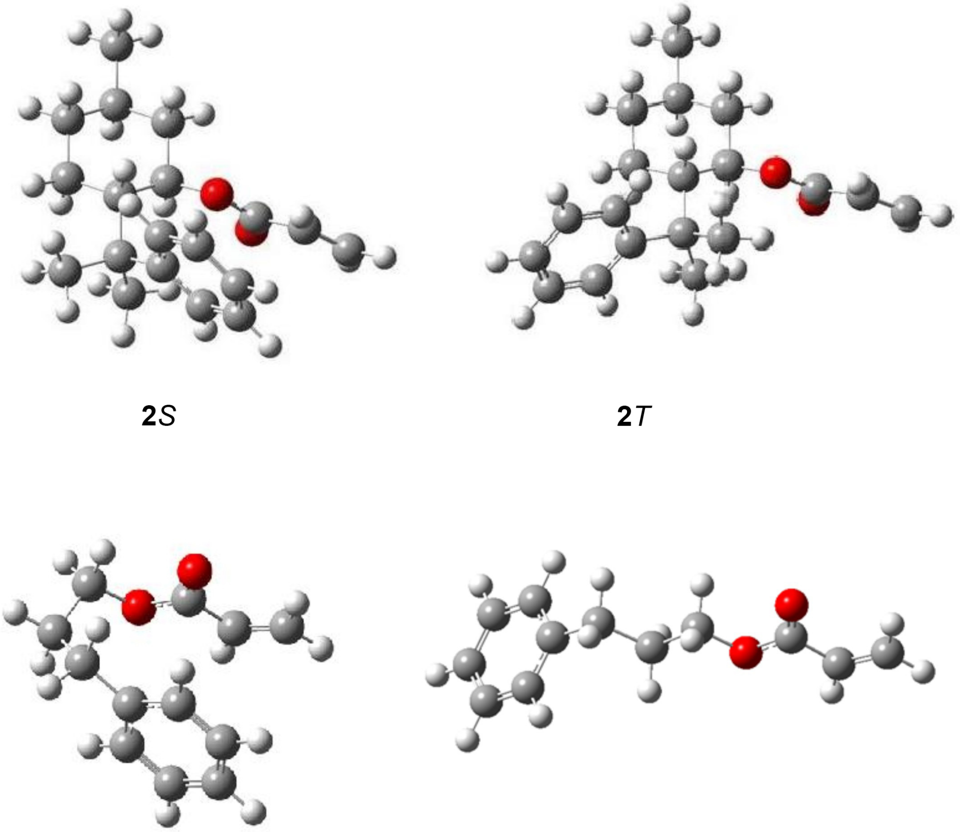

2*S* **2***T*

3*S* **3***T*

Figure 2. Local minima for the conformations **2***S*, **2***T*, **3***S* and **3***T* optimized in MPW1B95/6-311++G(2d,2p) theoretical level.

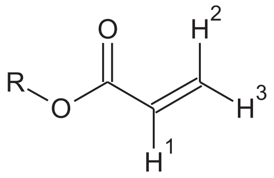

Figure 3. Representative structure for acrylate derivative **2**, **3** and **5**.

Table 1. 1H NMR data (in δ ppm) to methyl acrylate (R = CH_3),[34] 3-phenylpropylacrylate (R = 3-phenylpropyl)[35] and (+)-8-phenylmenthol acrylate (R = (+)-8-phenylmenthyl)[1]

Entry	R	H^1	H^2	H^3
1	methyl (**5**)	6.13	6.40	5.82
2	3-phenylpropyl (**3**)	6.10	6.39	5.77
3	(+)-8-phenylmenthyl (**2**)	5.59	6.01	5.57

the corresponding signals of H^1, H^2 and H^3 at higher field, which does not occur.

On the other hand, in the same Table 1, we observed an important shielding effect on the hydrogen atoms H^1, H^2 and H^3 in **2** compared with the corresponding hydrogen atoms H^1, H^2 and H^3 in **5** ($\Delta\delta$ = 0.46 ppm for H^1; 0.39 for H^2 and 0.25 for H^3). These data confirm that the conformation **2***S* is more stable that **2***T* on this equilibrium. We can note in Figure 2 that H^1, H^2 and H^3 in **2***S* are disposed in anisotropic shielding of the aromatic ring, modifying the corresponding signals to higher field.

As can be seen from Figure 2, there are no steric effects in **3T** between the benzylic and acrylate moieties due to the existence of the two hydrogen atoms in benzylic position. Thus, we have selected the molecule 3-phenylpropylacrylate (**3**) as a good model to indirectly evaluate the π–π stacking effect without the presence of steric effects observed in **2**. From this point of view, an efficient theoretical method has to corroborate these experimental data.

Initially, we have performed geometry optimizations for the ground states of the conformers **2***T*, **2***S* using HF method with the basis set 6-311++G(2d,2p) considering Cartesian *d* functions for polarization. We have found $\Delta\varepsilon_{2S-2T}$ = 0.00 kcal mol^{-1} for relative total energy for these conformations. This finding confirms that the Hartree-Fock method underestimate the π–π stacking interaction, in discordance to the ^{1}H NMR data which show the **2***S* conformation is more stable than **2***T*. This result was already expected since the *ab initio* Hartree-Fock method does not consider electron correlation and it cannot accurately measure the π–π stacking interactions. Thus, this method is more appropriate to evaluate the steric effect contributions than π–π stacking.

Then we have performed geometry optimizations for the ground states of conformers **3***T*, **3***S* using MP2 method and the same basis set. We have found $\Delta\varepsilon_{3S-3T} = -2.73$ kcal mol^{-1} for the relative total energy for these conformations. This finding also confirms that the MP2 method overestimate the π–π stacking interaction, in discordance to the ^{1}H NMR data which show the **3***T* conformation is more stable than **3***S*.

As a preliminary conclusion, neither Hartree-Fock nor MP2 are good methods to study the conformational equilibria for these compounds.

On these grounds, we have decided to investigate the efficiency of some recent DFT methods to describe the conformational equilibria for the molecules **2** and **3**.

So, we have used the DFT methods MPW1B95, M06, M06-2X and B97D with the same basis set to find the ground state minima for **2***T*, **2***S*, **3***T* and **3***S* conformations.

Table 2 shows gas phase relative total energies ($\Delta\varepsilon$), gas phase relative total energies including thermal corrections ($\Delta\varepsilon^{thermal}$) and gas phase relative Gibbs energy ($\Delta G°$, T = 298.15K and p = 1.0 atm) to (+)-8-phenylmenthyl acrylate (**2**) *trans* (**2***T*) and stacking (**2***S*) conformations, and to 3-phenylpropylacrylate (**3**) *trans* (**3***T*) and stacking (**3***S*) conformation (values in kcal mol^{-1}) using the following DFT methods: MPW1B95, M06, M06-2X and B97D. Table 2 still shows the relative conformational populations (in percentage) corresponding to $\mathbf{3}T \rightleftharpoons \mathbf{3}S$ inter-conversion equilibrium. Conformational equilibrium population **[3***T***]** can be evaluated from the equilibrium constant expression using the well-known equation (equation 1).

$$[3\mathrm{T}] = \frac{1}{1+\exp\left(-\Delta G_{3\mathrm{S}-3\mathrm{T}}/RT\right)} \qquad (1)$$

The conformational equilibrium population for **3***S* can be easily obtained keeping in mind that [**3***S*] = 1 – [**3***T*].

Negative values for $\Delta\varepsilon$, $\Delta\varepsilon^{thermal}$ and ΔG properties indicate that the conformation stacking (*S*) is preferable to the corresponding *trans* (*T*) conformation and the positive one indicate the *trans* conformation (*T*) as the preferable in such equilibrium.

From both calculated $\Delta\varepsilon$, $\Delta\varepsilon^{thermal}$ results it can be seen that the MPW1B95 is the only DFT method capable to correctly predict the relative stability between the studied conformations of molecules **2** and **3**. Indeed, this theoretical method predicts that the **2***S* is the most stable conformer in the conformational equilibrium for **2** and **3***T* is the most stable conformer in the conformational equilibrium for **3**, corresponding to negative $\Delta\varepsilon_{2S-2T}$ and $\Delta\varepsilon^{thermal}_{2S-2T}$ and positive $\Delta\varepsilon_{3S-3T}$ and $\Delta\varepsilon^{thermal}_{3S-3T}$ values.

Our results for gas phase relative Gibbs energies show that the M06 and B97D methods incorrectly predict the conformational equilibrium for the molecule **2** ($\Delta G_{2S\text{-}2T} > 0$), indicating a lacking of π–π stacking interaction on its conformational equilibrium in contrast to ^{1}H NMR experimental values shown in Table 1.

Based in the results for Gibbs energies, both DFT methods, M06-2X and MPW1B95 correctly predict the conformational equilibria for compounds **2** and **3** ($\Delta G_{2S\text{-}2T} < 0$ and $\Delta G_{3S\text{-}3T} > 0$). However, the value of $\Delta G_{3S\text{-}3T} = +0.72$ kcal mol^{-1} calculated using M06-2X method results in the equilibrium population for **3S** of 22.88%. Considering this population on the conformational equilibrium of the molecule **3**, ^{1}H NMR data through its anisotropic shielding would show the existence of stacking conformation and this evidence is not observed from the data presented in Table 1. On the other hand, MPW1B95 predicts $\Delta G_{3S\text{-}3T} = +4.41$ kcal mol^{-1}, corresponding to [**3***T*] = 99.94% for the *trans* conformation of this molecule. These results are fully consistent with the experimental observations: a complete lacking of anisotropic shielding in the ^{1}H NMR spectra of **3**, as we can see in Table 1.

From these results, we have considered the MPW1B95 method to be the most efficient in correctly describing conformational equilibria of molecules **2** and **3**. For this reason, on the following steps of our study we have decided to verify which methods produce gas phase relative total energies for **2** and **3** conformers in accordance with experimental data. So, we have carried out single

Table 2. Calculated gas phase relative total energies ($\Delta\varepsilon$), gas phase relative total energies including thermal corrections ($\Delta\varepsilon^{thermal}$) and gas phase relative Gibbs energy (ΔG, T = 298.15 K and p = 1.0 atm), all in kcal mol^{-1}, for **2***S*–**2***T* and **3***S*–**3***T* conformers and the relative conformational population (in percentage) for **3***S*–**3***T* conformers

Method	$\Delta\varepsilon_{2S-2T}$	$\Delta\varepsilon_{3S-3T}$	$\Delta\varepsilon^{thermal}_{2S-2T}$	$\Delta\varepsilon^{thermal}_{3S-3T}$	ΔG_{2S-2T}	ΔG_{3S-3T}	%[**3***S*]	%[**3***T*]
MPW1B95	−0.59	+1.24	−0.63	+1.55	−0.39	+4.41	0.06	99.94
M06	−1.45	−0.67	−1.02	−0.68	+0.22	+1.27	10.49	89.51
M06-2X	−1.46	−0.82	−1.49	−1.04	−0.97	+0.72	22.88	77.12
B97D	−1.55	−0.72	−1.26	−0.68	+0.16	+0.27	38.80	61.20

point energy calculation using MPW1B95 ground state geometries.

This same strategy was carried out by Swart *et al.*[14] and Moa *et al.*,[15] where they have used a theoretically predicted conformation from a reference method in order to evaluate several different computational methods performing single point calculations.

In Table 3 we present gas phase relative total energies obtained from single point calculations to **2***T* and **2***S* ($\Delta\varepsilon^{SP}_{2S-2T}$), and to **3***T* and **3***S* ($\Delta\varepsilon^{SP}_{3S-3T}$) considering several *ab initio* and DFT methods.

Table 3. Single point gas phase relative total energies ($\Delta\varepsilon^{SP}$) (in kcal mol^{-1}) for **2***S*–**2***T* and **3***S*–**3***T* conformers using several methodologies calculated at the MPW1B95/6-311++G(2d,2p) minimum geometries

Entry	Method	$\Delta\varepsilon^{SP}_{2S-2T}$	$\Delta\varepsilon^{SP}_{3S-3T}$
1	HF	+0.50	+5.74
2	MP2	−1.89	−2.40
3	SCS-MP2	−1.38	−0.85
4	MP3	−0.93	+0.34
5	SCS-MP3	−1.16	−0.17
6	LSDA	−0.96	−1.26
7	B3LYP	+0.42	+4.19
8	B3LYP-D	−1.29	−0.61
9	B3PW91	+0.35	+4.08
10	HCTH	+0.42	+4.80
11	MW1PW91	+0.16	+3.48
12	PBE1PBE	−0.06	+2.84
13	MPWB1K	−0.70	+0.98
14	MPW1B95	−0.59	+1.24
15	M06	−1.21	−0.63
16	M06-2X	−1.30	−0.53
17	B97D	−1.33	−0.78

In Table 3 we can observe that HF method predicts total energy for **3***T* 5.74 kcal mol^{-1} lower than **3***S* (entry 1). On the other hand, **2***T* and **2***S* conformations have similar energies ($\Delta\varepsilon^{SP}_{2S-2T} = +0.50$ kcal mol^{-1}). These results indicate that there is no steric effect between the benzylic hydrogen atoms and the acrylate moiety on **3***T* conformation (see Figure 2). Differently, there is a steric effect between one of the benzylic methyl groups and the acrylate moiety on the **2***T* conformation and a steric effect between phenyl and acrylate groups in the **2***S* conformation. So, considering only the steric effects, the energies of **2***T* and **2***S* are almost equal. Thus, any method capable to catch π–π stacking interaction effects should indicate more stability for the **2***S* than **2***T*.

The DFT methods: LSDA, B3LYP-D, MPW1BK, MPW1B95, M06, M06-2X and B97D indicates that **2***S* is lower in energy than **2***T* (see Table 3). The a*b initio* methods MP2, MP3 and their spin-component–correction versions (SCS-MP2 and SCS-MP3) also indicate conformation **2***S* as the most stable. The DFT methods B3LYP, B3PW91, HCTH and MPW1PW91 were not efficient to estimate π–π stacking interaction on **2**.

Differently from the analysis for **2**, LSDA, MP2, B97D and B3LYP-D methods show erroneously that the conformation **3***S* is more stable than **3***T*. Surprisingly, spin-component-correction versions of both MP2 and MP3 erroneously predicted conformation **3***S* as the most stable. Since ^{1}H NMR experimental data in Table 1 confirms that conformation **3***S* is not more stable than **3***T* on the equilibrium, this evidence points out that LSDA, B3LYP-D, B97D, MP2, SCS-MP2 and SCS-MP3 methods are overestimating the π–π stacking effect in this case.

In fact, as reported by Moa *et al.*,[15] the Truhlar's DFT methods MPWB1K and MPW1B95 were efficient methods to count the contribution of the π–π stacking effects for compounds **2** and **3**. The same results were observed when we used MP3 method to calculate gas phase relative total energy. However, MP3 calculations for large molecules are of prohibitive computational expense.

Calculation of NMR chemical shifts can be used to bring forth more information about conformational equilibria for compounds **2** and **3**.

For this, we have carried out proton chemical shift calculations using gauge invariant atomic orbital (GIAO) methodology[43] and MPW1B95 gas phase ground state geometries considering solvent effects through PCM model.[44] These results are presented in Table 4. The hydrogen atoms shown in table 4 are the same highlighted in Figure 3 and their experimental ^{1}H NMR chemical shifts data are in Table 1.

Table 4. Predicted ^{1}H NMR chemical shifts (in ppm) for **2***T*, **2***S*, **3***T* and **3***S* conformers using GIAO MPW1B95/6-311++G(2d,2p) and PCM continuum model (the solvent was set as chloroform). The hydrogen atoms shown in this table are the same as shown in Table 1 and Figure 3

Entry	Conformer	H^1	H^2	H^3
1	**2***S*	5.42	7.05	6.13
2	**2***T*	6.77	7.27	6.45
3	**3***S*	5.51	6.85	5.87
4	**3***T*	6.70	7.30	6.40

A comparison between the predicted chemical shifts and the corresponding experimental ones (respectively, Table 4 and Table 1) show that, despite this non quantitative concordance, we can see the same trends between these data. As it should be expected, all hydrogen atoms for conformation **2***S* become more shielded than the corresponding ones in conformation **2***T*. This same evidence could be observed for the hydrogen atoms of the molecule **3**.

In a last step, we have decided to predict the minimum geometry of the benzene···methyl-acrylate complex **4** (Figure 4) in order to measure the π–π stacking without steric interferences. For this calculation we have used MPW1B95/6-311G++(2d,2p) (with Cartesian *d* functions for polarization atomic orbitals) which was the best theoretical method to study these compounds. In this part, our goal was to accurately measure the total formation energy (ΔE^{cs}) for this complex where the benzene and methyl acrylate are in parallel position to each other, as occurs in **2***S*.

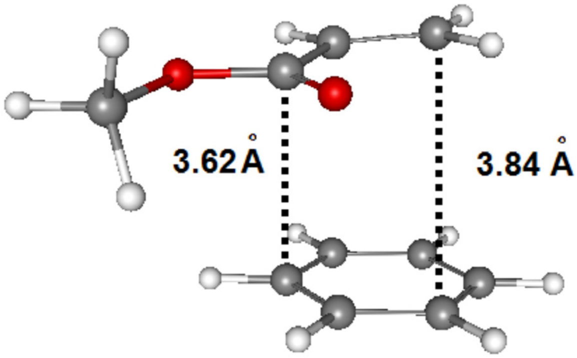

Figure 4. Optimized geometry of the benzene···methyl-acrylate complex **4** using MPW1B95/6-311++G(2d,2p) level of theory.

Note that in complex **4** there are no relevant steric interactions such as the ones in **2**, so the calculated value of the ΔE^{cs} serve as a good estimation to the dispersion effects that occur in the conformation **2***S*.

The calculated π–π stacking energy ΔE^{cs} for this complex **4** (Figure **4**) was −1.30 kcal mol^{-1} (−0.95 kcal mol^{-1}, considering the BSSE correction = 0.35 kcal mol^{-1})[49] (Table 5). Considering the relative total energies of all conformers of **2** and **3** (Tables 2 and 3), we believe that this π–π stacking stabilization energy is not large enough to overcome the larger stability of the **3***T* conformation in comparison to **3***S*, due to the inexistence of steric effects on **3***T*.

Table 5. Total energy (E), uncorrected stacking energy (ΔE^{s}), BSSE amounts and corrected stacking energy (ΔE^{cs}) the benzene···methyl-acrylate (Bz-MA) complex at the MPW1B95 level of theory[a]

Entry	R	E	ΔE^{s}	BSSE	ΔE^{cs}
1	MA	−306.43239576	-	-	-
2	Bz	−232.19609799	-	-	-
3	Bz···MA	−538.63055147	−1.3	0.35	−0.95

[a]Values of E are given in Hartree and values of ΔE^{s}, BSSE and ΔE^{cs} are given in kcal mol^{-1}.

The observation that $\Delta\varepsilon_{2S-2T}$ = 0.00 kcal mol^{-1} (obtained by HF//HF) and $\Delta\varepsilon_{2S-2T}$ = +0.50 kcal mol^{-1} (obtained by HF//MPW1B95) points out that the steric effects on **2***T* and **2***S* are practically the same. Therefore the obtained value of −0.95 kcal mol^{-1} suggests that the dispersion contribution is crucial for the relative stability of the conformation **2***S* on the conformational equilibrium of **2**.

Conclusions

The study described in the present manuscript was performed by applying nearly two dozen different quantum chemical to calculate local minimum geometries, frequencies, thermochemical properties and ^{1}H NMR chemical shifts for (+)-8-phenylmentyl acrylate (**2**) and 3-phenylpropyl acrylate (**3**). These calculations were applied aiming to revisit the origin of the preferential π–π stacking conformation of the **2**.

Based on our theoretical results we have presented more evidences that point neither Hartree-Fock nor Møller-Plesset perturbation theory (MP2) methods as able to accurately treat π–π stacking interactions (respectively, underestimating and overestimating these effects).

Additionally, we have a clear proof that, differently than what were observed by Swart *et al.*,[14] the LSDA functional indeed overestimates π–π stacking interaction in these molecules (**2** and **3**) as well as the recent DFT methods B97D, M06 and M06-2X which were developed to treat dispersion effects.

Our results from Gibbs energies and equilibrium populations for stacking and *trans* conformations of **2** and **3** show that the MPW1B95 is really the most suitable method to evaluate the contributions between the π–π stacking and steric effects, as were reported by Moa *et al.*[15]

We believe that considering the dispersion π-π stacking interactions as the only origin to the high efficiency of **2** for asymmetric reactions is not correct. Two pivotal effects (the repulsive steric and attractive π–π stacking dispersion) have to be considered for the analysis of the origin of the great efficiency of **2** in asymmetric reactions.

The steric effect between the benzylic methyl group and the acrylate moiety in **2** disfavors the **2***T* conformer in comparison to **2***S***.** At same time, the steric effect between phenyl and acrylate groups disfavors the **2***S* conformation in comparison to **2***T*. These two opposite steric effects seem to be compensated by each other.

On the other hand, because of the stabilizing π–π stacking intramolecular interaction between the phenyl group and acrylate moiety, the **2***S* conformer is favored in comparison to **2***T*. Then, there is a balance of these two effects (dispersion and steric), favoring the **2***S* conformation.

The π–π stacking interaction is really decisive (but not the only effect) to lead **2***S* as the more important conformer in equilibrium of (+)-8-phenylmentyl acrylate (**2**).

We believe that the calculated π–π stacking interaction energy for the intermolecular benzene···acrylate complex **4** (−0.95 kcal mol^{-1}) could be used to estimate the intramolecular π–π stacking interactions on **2***S* and **3***S*. This energy is large enough to shift the conformational equilibrium to **2***S*. However, it is not strong enough to make **3***S* conformation the most stable.

We hope that this study can provide new insights to rational design of new chiral auxiliaries for enantioselective synthesis.

Supplementary Information

Supplementary data are available free of charge at http://jbcs.sbq.org.br, as PDF file.

Acknowledgments

We would like to thank FAPESQ (Fundação de Amparo à Pesquisa do Estado da Paraíba), CNPq (Conselho Nacional de Desenvolvimento Científico e Tecnológico) and INCT-INAMI (Instituto Nacional de Ciência e Tecnologia de Nanotecnologia para Marcadores Integrados). We also thank to G. A. U. Carvalho for reviewing our manuscript in English.

References

1. Corey, E. J.; Ensley, H. E.; *J. Am. Chem. Soc.* **1975**, *97*, 6908.
2. See In: Ager, D., *Handbook of Chiral Chemicals*, S. Ed.; CRC press Taylor & Francis group : New York; T; 2006.
3. Mezrhab, B.; Dumas, F.; d'Angelo, J.; Riche, C.; *J. Org. Chem.* **1994**, *59*, 500.
4. Ulukanli, S; Karabuga, S; Celik, A.; Kazaz, C.; *Tetrahedron Lett.* **2005**, *46*, 197.
5. Actually, aliphatic molecules like long alkanes chains also involve some dispersion effect. Our analysis is approximated. Please consult the following reference for additional understanding Grime S.; Schwabe, T.; *Phys. Chem. Chem. Phys.* **2007**, *9*, 3397.
6. Hobza, P.; *Phys. Chem. Chem. Phys.* **2008**, *10*, 2581.
7. Cerný, J.; Hobza, P.; *Phys. Chem. Chem. Phys.* **2007**, *9*, 5291.
8. Zhao, Y.; Truhlar, D. G.; *J. Chem. Theory Comput.* **2009**, *4*, 1849.
9. Sinnokrot, M. O.; Sherrill, C. D.; *J. Phys. Chem. A* **2006**, *110*, 10656.
10. Hobza, P.; Selzle, H.L.; Schlag, E.W.; *J. Phys. Chem.* **1996**, *100*, 18790.
11. Tsuzuki, S.; Uchimaru, T.; Matsumura, K.; Mikami, M.; Tanabe, K.; *Chem. Phys. Lett.* **2000**, *319*, 547.
12. Zhao, Y.; Truhlar, D.; *J. Chem. Theory Comput.* **2005**, *1*, 415.
13. Zhao, Y.; Truhlar, D. G.; *Acc. Chem. Res.* **2008**, *41*, 157.
14. Swart, M.; van der Wijst, T.; Guerra, C. F.; Bickelhaupt, F. M.; *J. Mol. Model.* **2007**, *13*, 1245.
15. Moa, M. J. G.; Mandado, M.; Mosquera, R.; *J. Phys. Chem. A* **2007**, *111*, 1998.
16. Costa, P. R. R.; Cabral, L. M.; Alencar, K. G.; Schmidt, L. L.; Vasconcellos, M. L. A. A.; *Tetrahedron Lett.* **1997**, *38*, 7021.
17. Vasconcellos, M. L. A. A.; Mellão, M.; *Tetrahedron: Asymmetry* **1996**, *7*, 1607.
18. Alencar, K. G.; Dumas, F., Costa, P. R. R.; Vasconcellos, M. L. A. A.; *Tetrahedron: Asymmetry* **1997**, *8*, 579.
19. Vasconcellos, M. L. A. A.; Miranda, L. S.; Leitão, M., S. G.; Fernandes, P. D.; Marinho, B. G.; Matheus, M. E.; *Bioorg. Med. Chem. Lett.* **2004**, *14*, 1573.
20. Lima Filho, U. F.; Vasconcellos, M. L. A. A.; Pinheiro, S.; Costa, P. R. R.; *Tetrahedron: Asymmetry* **1994**, *5*, 1219.
21. de Souza, R. O. M. A.; Meireles, B. A.; Aguiar, L. C. S.; Vasconcellos, M. L. A. A.; *Synthesis*, **2004**, 1595.
22. Filho, E. B. A.; Ventura, E.; do Monte, S. A.; Oliveira, B. G.; Junior, C. G. L.; Rocha G. B.; Vasconcellos, M. L. A. A.; *Chem. Phys. Lett.* **2007**, *449*, 336.
23. Vasconcellos, M. L. A. A.; Silva, T. M. S.; Camara, C.A.; Martins, R.M.; Lacerda, K. M.; Lopes, H. M.; Pereira, V. L. P.; de Souza, R. O. M. A.; Crespo, L.T.C.; *Pest Manage.Sci*. **2006**, *62*, 288.
24. de Souza, R. O. M. A.; Pereira, V. L. P.; Muzitano, M. F.; Falcão, C. A. B.; Rossi-Bergmann, B.; Filho, E. B. A.; Vasconcellos, M. L. A. A.; *European J. Med. Chem.* **2007**, *42*, 99.
25. Barbosa, T. P.; Junior, C. G. L.; Silva, F. P. L.; Lopes, H. M.; Figueiredo, R. L. F; Sousa, S. C. O.; Batista, G. N.; da Silva, T. G; Silva, T. M. S; Oliveira, M. R.; Vasconcellos, M. L. A. A.; *European J. Med. Chem.* **2009**, *44*, 1726.
26. Zhao, Y.; Truhlar, D. G.; *J. Phys. Chem. A* **2004**, *108*, 6908.
27. Zhao, Y.; Truhlar, D. G.; *Theor. Chem. Acc.* **2008**, 120, 215.
28. Grimme, S.; *J. Comp. Chem.* **2006**, 27, 1787.
29. Kohn, W.; Sham, L.; *J. Phys. Rev.* **1965**, *140*, A1133.
30. Becke, A. D.; *J. Chem. Phys.* **1993**, *98*, 5648.
31. Sousa, S. F.; Fernandes, P. A.; Ramos, M. J.; *J. Phys. Chem. A*, **2007**, *111*, 10439.
32. Grimme, S.; *J. Comput. Chem.* **2004**, *25*, 1463.
33. Becke, A. D.; *Phys. Rev. A: At., Mol., Opt. Phys.* **1988**, *38*, 3098.
34. Adamo, C.; Barone, V.; *J. Chem. Phys.* **1998**, *108*, 664.
35. Hamprecht, F. A.; Cohen, A. J.; Tozer, D. J.; Handy, N. C.; *J. Chem. Phys.* **1998**, *109*, 6264.
36. Perdew, J. P.; Burke, K.; Ernzerhof, M.; *Phys. Rev. Lett.* **1997**, *78*, 1396.
37. Lynch B. J.; Fast, P. L.; Harris, M.; Truhlar, D. G.; *J. Phys. Chem. A* **2000**, *104*, 4811.

38. Grimme, S.; *J. Chem. Phys.* **2003**, *118***,** 9095**.**
39. Grimme, S.; *J. Comput. Chem.* **2003**, *24*, 1529.
40. Frisch, M. J.; Trucks, G. W.; Schlegel, H. B.; Scuseria, G. E.; Robb, M. A.; Cheeseman, J. R.; Montgomery, Jr., J. A.; Vreven, T.; Kudin, K. N.; Burant, J. C.; Millam, J. M.; Iyengar, S. S.; Tomasi, J.; Barone, V.; Mennucci, B.; Cossi, M.; Scalmani, G.; Rega, N.; Petersson, G. A.; Nakatsuji, H.; Hada, M.; Ehara, M.; Toyota, K.; Fukuda, R.; Hasegawa, J.; Ishida, M.; Nakajima, T.; Honda, Y.; Kitao, O.; Nakai, H.; Klene, M.; Li, X.; Knox, J. E.; Hratchian, H. P.; Cross, J. B.; Bakken, V.; Adamo, C.; Jaramillo, J.; Gomperts, R.; Stratmann, R. E.; Yazyev, O.; Austin, A. J.; Cammi, R.; Pomelli, C.; Ochterski, J. W.; Ayala, P. Y.; Morokuma, K.; Voth, G. A.; Salvador, P.; Dannenberg, J. J.; Zakrzewski, V. G.; Dapprich, S.; Daniels, A. D.; Strain, M. C.; Farkas, O.; Malick, D. K.; Rabuck, A. D.; Raghavachari, K.; Foresman, J. B.; Ortiz, J. V.; Cui, Q.; Baboul, A. G.; Clifford, S.; Cioslowski, J.; Stefanov, B. B.; Liu, G.; Liashenko, A.; Piskorz, P.; Komaromi, I.; Martin, R. L.; Fox, D. J.; Keith, T.; Al-Laham, M. A.; Peng, C. Y.; Nanayakkara, A.; Challacombe, M.; Gill, P. M. W.; Johnson, B.; Chen, W.; Wong, M. W.; Gonzalez, C.; Pople, J. A.; *Gaussian* 03, Revision C.02, Gaussian, Inc., Wallingford CT, 2004.
41. Frisch, M. J.; Trucks, G. W.; Schlegel, H. B.; Scuseria, G. E.; Robb, M. A.; Cheeseman, J. R.; Scalmani, G.; Barone, V.; Mennucci, B.; Petersson, G. A.; Nakatsuji, H.; Caricato, M.; Li, X.; Hratchian, H. P.; Izmaylov, A. F.; Bloino, J.; Zheng, G.; Sonnenberg, J. L.; Hada, M.; Ehara, M.; Toyota, K.; Fukuda, R.; Hasegawa, J.; Ishida, M.; Nakajima, T.; Honda, Y.; Kitao, O.; Nakai, H.; Vreven, T.; Montgomery, Jr., J. A.; Peralta, J. E.; Ogliaro, F.; Bearpark, M.; Heyd, J. J.; Brothers, E.; Kudin, K. N.; Staroverov, V. N.; Kobayashi, R.; Normand, J.; Raghavachari, K.; Rendell, A.; Burant, J. C.; Iyengar, S. S.; Tomasi, J.; Cossi, M.; Rega, N.; Millam, N. J.; Klene, M.; Knox, J. E.; Cross, J. B.; Bakken, V.; Adamo, C.; Jaramillo, J.; Gomperts, R.; Stratmann, R. E.; Yazyev, O.; Austin, A. J.; Cammi, R.; Pomelli, C.; Ochterski, J. W.; Martin, R. L.; Morokuma, K.; Zakrzewski, V. G.; Voth, G. A.; Salvador, P.; Dannenberg, J. J.; Dapprich, S.; Daniels, A. D.; Farkas, Ö.; Foresman, J. B.; Ortiz, J. V.; Cioslowski, J.; Fox, D. J.; *Gaussian* 09, Revision A.1, Gaussian, Inc., Wallingford CT, 2009.
42. Neese, F.; ORCA. An *Ab Initio*, Density Functional and Semiempirical Program Package, version 2.6.35L; University of Bonn: Bonn, Germany.
43. Cheeseman, J. R.; Trucks, G. W.; Keith, T. A.; Frisch, M. J.; *J. Chem. Phys.* **1996**, 104, 5497.
44. Tomasi, J.; Mennucci, B.; Cammi, R.; *Chem. Rev.* **2005**, 105, 2999.
45. Boys, S. F.; Bernardi, F.; *Mol. Phys.* **1970**, *19*, 553.
46. Schwenke, D. W.; Truhlar D.G.; *J. Chem. Phys.* **1985**, *82*, 2418.
47. SDBS, Spectral Database for Organic Compounds, http://riodb01.ibase.aist.go.jp/sdbs/, accessed in July 20, 2009.
48. Kim, J. H.; Eun-Soo, P.; Shim, J. H.; Mal-Nam, K.; Woong-Sik, M.; Kyoo-Hyun, C.; Jin-San, Y.; *J. Agric. Food. Chem.* **2004**, *52*, 7480.
49. Curiously, in the Truhlar's paper (see reference 12 and 13) and quinhydrone complex calculation (see reference 15) the BSSE correction were not performed. However, we are sure that the kind of correction is pivotal to obtain accuracy of the calculation.

Submitted: September 23, 2009

J. Braz. Chem. Soc., Vol. 21, No. 9, S1-S6, 2010.
Printed in Brazil - ©2010 Sociedade Brasileira de Química
0103 - 5053 $6.00+0.00

Revisiting the Origin of the Preferential π–π Stacking Conformation of the (+)–8–Phenylmenthyl Acrylate

Saulo L. Capim, Sidney R. Santana, Boaz G. de Oliveira, Gerd B. Rocha* and Mário L. A. A. Vasconcellos*

*Departamento de Química, Universidade Federal da Paraíba, Campus I,
58059–900 João Pessoa–PB, Brazil*

Table S1. Cartesian coordinates and energies of HF/6–311++G(2d,2p) geometry optimized structures 2 and 3 (conformations **2***S*, **2***T*,**3***S* and **3***T*).

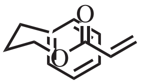

Stacking (*S*)

3*S*

Standard orientation: opt RHF/6–311++g(2d,2p)6d
E = −612.47937340 a.u.

Center Number	Atomic Number	Atomic Type	Coordinates (Angstroms)		
			X	Y	Z
1	6	0	1.205188	1.945146	–0.015940
2	6	0	–0.137280	2.498597	–0.450446
3	6	0	–1.349391	2.064574	0.386618
4	6	0	2.366553	–0.088480	–0.022114
5	6	0	2.292837	–1.508206	–0.456294
6	8	0	3.275064	0.398184	0.564463
7	6	0	3.295279	–2.331948	–0.241203
8	6	0	–1.782755	0.621205	0.244542
9	6	0	–2.356035	0.168010	–0.936100
10	6	0	–2.763168	–1.143724	–1.071673
11	6	0	–2.610096	–2.032474	–0.021770
12	6	0	–2.050434	–1.592011	1.160281
13	6	0	–1.643202	–0.275330	1.289776
14	1	0	1.348487	2.041734	1.050826
15	1	0	2.009272	2.474791	–0.505628
16	1	0	–0.294792	2.262492	–1.496072
17	1	0	–0.061957	3.578950	–0.384358
18	1	0	–2.182964	2.699761	0.108767
19	1	0	–1.146249	2.273135	1.430401
20	1	0	1.390096	–1.815774	–0.944390
21	1	0	3.248347	–3.357345	–0.552214
22	1	0	4.185885	–1.995478	0.252300
23	1	0	–2.488522	0.846560	–1.758011
24	1	0	–3.204807	–1.471878	–1.992862
25	1	0	–2.929383	–3.051294	–0.124166
26	1	0	–1.930842	–2.268921	1.984078
27	1	0	–1.209951	0.052017	2.215888
28	8	0	1.282736	0.574203	–0.374292

Table S2. Cartesian coordinates and energies of HF/6–311++G(2d,2p) geometry optimized structures 2 and 3 (conformations **2***S*, **2***T*, **3***S* and **3***T*).

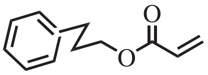

Trans (*T*)

3*T*

Standard orientation: opt RHF/6–311++g(2d,2p)6d
E = −612.48328199 a.u.

Center Number	Atomic Number	Atomic Type	Coordinates (Angstroms)		
			X	Y	Z
1	6	0	–1.391617	0.722918	–0.002296
2	6	0	–0.033663	0.054653	–0.000267
3	6	0	1.100880	1.083531	–0.003888
4	6	0	–3.643853	0.077859	–0.000295
5	6	0	–4.556002	–1.095844	0.003549
6	8	0	–3.993900	1.210135	–0.004088
7	6	0	–5.861439	–0.935776	0.003433
8	6	0	2.471488	0.446802	–0.001633
9	6	0	3.111800	0.141229	1.189866
10	6	0	4.353261	–0.466711	1.194760
11	6	0	4.978808	–0.778992	0.002733
12	6	0	4.352938	–0.475935	–1.191447
13	6	0	3.111436	0.132050	–1.190880
14	1	0	–1.529032	1.341280	–0.877672
15	1	0	–1.528901	1.346849	0.869141
16	1	0	0.050052	–0.588362	–0.868197
17	1	0	0.050333	–0.582573	0.871892
18	1	0	1.004604	1.727822	0.862534
19	1	0	1.004606	1.721675	–0.874849
20	1	0	–4.097690	–2.064295	0.006406
21	1	0	–6.524830	–1.778501	0.006175
22	1	0	–6.293519	0.045630	0.000474
23	1	0	2.639555	0.383780	2.123417
24	1	0	4.832048	–0.691979	2.128058
25	1	0	5.943407	–1.247769	0.004427
26	1	0	4.831422	–0.708395	–2.123135
27	1	0	2.638953	0.367385	–2.126158
28	8	0	–2.379253	–0.298541	0.001049

---

*e–mail: mlaav@quimica.ufpb.br, gbr@quimica.ufpb.br

Table S3. Cartesian coordinates and energies of HF/6–311++G(2d,2p) geometry optimized structures 2 and 3 (conformations **2***S*, **2***T*,**3***S* and **3***T*).

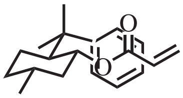

Stacking (*S*)

2*S*

Standard orientation: : opt RHF/6–311++g(2d,2p) 6d
E = −884.62474366 a.u.

Center Number	Atomic Number	Atomic Type	Coordinates (Angstroms)		
			X	Y	Z
1	6	0	2.225330	–1.804189	0.366358
2	6	0	3.425739	–1.320553	–0.445397
3	6	0	3.664485	0.177400	–0.290432
4	6	0	2.378738	0.925684	–0.628427
5	6	0	1.193801	0.443615	0.199221
6	6	0	0.923313	–1.055714	0.017136
7	6	0	–0.339122	–1.597926	0.784647
8	6	0	–0.330827	–3.144055	0.815190
9	6	0	–0.329079	–1.127830	2.247581
10	6	0	–1.644825	–1.199000	0.065059
11	6	0	–1.840774	–1.541425	–1.270719
12	6	0	–3.018916	–1.256581	–1.928045
13	6	0	–4.054440	–0.621999	–1.265211
14	6	0	–3.884503	–0.284615	0.059397
15	6	0	–2.696603	–0.571091	0.713418
16	6	0	4.837349	0.664696	–1.134985
17	8	0	0.041905	1.179819	–0.209186
18	1	0	2.099684	–2.860893	0.188895
19	1	0	2.448169	–1.692302	1.422721
20	1	0	4.308538	–1.873626	–0.143204
21	1	0	3.264269	–1.547622	–1.496626
22	1	0	3.901107	0.372592	0.753394
23	1	0	2.505939	1.987396	–0.460637
24	1	0	2.143025	0.792374	–1.680495
25	1	0	1.380899	0.661064	1.237375
26	1	0	0.750046	–1.216088	–1.039793
27	1	0	–1.279103	–3.501880	1.193643
28	1	0	–0.189518	–3.570901	–0.169325
29	1	0	0.446763	–3.525560	1.462335
30	1	0	–1.116613	–1.612537	2.809628
31	1	0	–0.457596	–0.060180	2.349765
32	1	0	0.606760	–1.393650	2.719957
33	1	0	–1.067547	–2.043080	–1.817294
34	1	0	–3.130017	–1.534900	–2.958477
35	1	0	–4.973225	–0.401434	–1.772700
36	1	0	–4.674029	0.205689	0.595885
37	1	0	–2.610304	–0.285507	1.740350
38	1	0	5.008376	1.725220	–0.992823
39	1	0	5.750318	0.142933	–0.872338
40	1	0	4.652451	0.497359	–2.190902
41	6	0	–0.216884	2.340085	0.358913
42	6	0	–1.417403	2.975189	–0.247236
43	8	0	0.424602	2.812875	1.238687
44	1	0	–1.931560	2.411781	–0.999071
45	1	0	–2.674169	4.635909	–0.303190
46	6	0	–1.811556	4.170975	0.132933
47	1	0	–1.277642	4.710285	0.890522

Table S4. Cartesian coordinates and energies of HF/6–311++G(2d,2p) geometry optimized structures 2 and 3 (conformations **2***S*, **2***T*,**3***S* and **3***T*).

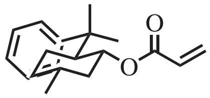

Trans (*T*)

2*T*

Standard orientation: HF/6–311++G(2d,2p) 6d
E = −884.62473753 a.u.

Center Number	Atomic Number	Atomic Type	Coordinates (Angstroms)		
			X	Y	Z
1	6	0	0.751393	1.679884	0.504564
2	6	0	0.112285	2.956074	–0.034386
3	6	0	–1.392536	2.980079	0.206987
4	6	0	–2.007975	1.708196	–0.366647
5	6	0	–1.360612	0.435459	0.170674
6	6	0	0.150415	0.393423	–0.099328
7	6	0	0.918924	–0.897455	0.373339
8	6	0	0.667307	–1.179572	1.862422
9	6	0	0.481660	–2.164665	–0.398369
10	6	0	2.420359	–0.704861	0.075366
11	6	0	3.391935	–0.685531	1.063221
12	6	0	4.734672	–0.525628	0.755933
13	6	0	5.141074	–0.379532	–0.551642
14	6	0	4.186087	–0.398683	–1.553071
15	6	0	2.852850	–0.561106	–1.241740
16	6	0	–2.053122	4.229492	–0.366427
17	8	0	–2.001121	–0.667199	–0.479113
18	1	0	1.812406	1.708516	0.314225
19	1	0	0.632879	1.663940	1.583223
20	1	0	0.580386	3.816757	0.430950
21	1	0	0.305965	3.037773	–1.101291
22	1	0	–1.558327	2.978384	1.282224
23	1	0	–3.067140	1.670405	–0.146388
24	1	0	–1.905661	1.711335	–1.448246
25	1	0	–1.552999	0.358100	1.227382
26	1	0	0.273288	0.452154	–1.175752
27	1	0	1.206474	–2.063900	2.176874
28	1	0	0.963803	–0.363851	2.506582
29	1	0	–0.382267	–1.371031	2.035130
30	1	0	1.201633	–2.954567	–0.225727
31	1	0	0.423821	–1.995286	–1.464599
32	1	0	–0.481460	–2.517646	–0.070018
33	1	0	3.122153	–0.790842	2.092780
34	1	0	5.457714	–0.515488	1.548762
35	1	0	6.179127	–0.255156	–0.790699
36	1	0	4.480531	–0.289933	–2.579211
37	1	0	2.142767	–0.575149	–2.044165
38	1	0	–3.117337	4.239981	–0.162035
39	1	0	–1.623909	5.127861	0.061752
40	1	0	–1.921482	4.280267	–1.442183
41	6	0	–3.101857	–1.169420	0.043025
42	6	0	–3.644199	–2.264819	–0.805177
43	8	0	–3.592030	–0.801585	1.058768
44	1	0	–3.103537	–2.495925	–1.700880
45	1	0	–5.132483	–3.699828	–1.066877
46	6	0	–4.737208	–2.909479	–0.459045
47	1	0	–5.259847	–2.657736	0.442762

Table S5. Cartesian coordinates and energies of HF/6–311++G(2d,2p) geometry optimized structures 2 and 3 (conformations **2***S*, **2***T*,**3***S* and **3***T*).

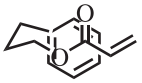

Stacking (*S*)

3*S*

Standard orientation: opt MP2/6–311++g(2d,2p) 6d
E = –614.68988216 a.u.

Center Number	Atomic Number	Atomic Type	Coordinates (Angstroms)		
			X	Y	Z
1	6	0	–2.716864	0.048546	–0.301562
2	6	0	–2.326814	–1.413931	–0.211465
3	6	0	–1.190743	–1.715953	0.770320
4	6	0	–0.845288	1.478996	0.006501
5	6	0	0.305841	2.073205	–0.706862
6	8	0	–1.052387	1.546940	1.201535
7	6	0	1.291319	2.657562	–0.019283
8	6	0	0.199580	–1.283801	0.356375
9	6	0	0.670988	–1.445629	–0.951931
10	6	0	1.984946	–1.116414	–1.288035
11	6	0	2.856300	–0.623387	–0.316695
12	6	0	2.398486	–0.451926	0.989797
13	6	0	1.082658	–0.779256	1.317609
14	1	0	–2.966351	0.452948	0.675748
15	1	0	–3.557250	0.183253	–0.976237
16	1	0	–2.085251	–1.783076	–1.207425
17	1	0	–3.215832	–1.959174	0.110600
18	1	0	–1.168200	–2.794532	0.937968
19	1	0	–1.422735	–1.258153	1.732747
20	1	0	0.328229	1.979662	–1.782053
21	1	0	2.152363	3.073364	–0.519652
22	1	0	1.235141	2.713982	1.058140
23	1	0	0.014336	–1.830553	–1.720437
24	1	0	2.327225	–1.251342	–2.305060
25	1	0	3.874938	–0.370816	–0.576051
26	1	0	3.061349	–0.064754	1.751569
27	1	0	0.728643	–0.628314	2.329235
28	8	0	–1.643744	0.824238	–0.873748

Table S6. Cartesian coordinates and energies of MP2/6–311++G(2d,2p) geometry optimized structures 3 (conformations **3***S* and **3***T*).

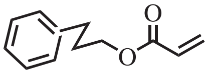

Trans (*T*)

3*T*

Standard orientation: opt MP2/6–311++g(2d,2p) 6d
E = –614.68553739 a.u.

Center Number	Atomic Number	Atomic Type	Coordinates (Angstroms)		
			X	Y	Z
1	6	0	1.375147	0.702327	–0.007998
2	6	0	0.008177	0.060489	–0.000146
3	6	0	–1.100321	1.116671	–0.013442
4	6	0	3.639497	0.061496	–0.000637
5	6	0	4.562645	–1.099159	0.014014
6	8	0	3.967100	1.230525	–0.016015
7	6	0	5.884445	–0.908442	0.010781
8	6	0	–2.463867	0.481861	–0.005976
9	6	0	–3.098174	0.137680	–1.204154
10	6	0	–4.338250	–0.500960	–1.200654
11	6	0	–4.962356	–0.806667	0.009285
12	6	0	–4.340936	–0.467193	1.211566
13	6	0	–3.100842	0.171344	1.199942
14	1	0	1.530383	1.334744	0.864259
15	1	0	1.530650	1.312681	–0.895779
16	1	0	–0.096586	–0.567407	0.884159
17	1	0	–0.096358	–0.589246	–0.868557
18	1	0	–0.992739	1.745930	–0.898178
19	1	0	–0.993226	1.767527	0.855580
20	1	0	4.122752	–2.084919	0.027130
21	1	0	6.569511	–1.741830	0.021278
22	1	0	6.283642	0.095198	–0.002546
23	1	0	–2.620742	0.378134	–2.146138
24	1	0	–4.816381	–0.754615	–2.136514
25	1	0	–5.924691	–1.298413	0.015101
26	1	0	–4.821145	–0.694573	2.153098
27	1	0	–2.625477	0.438079	2.135872
28	8	0	2.352826	–0.360270	0.005483

Table S7. Cartesian coordinates and energies of MP2/6–311++G(2d,2p) geometry optimized structures 3 (conformations **3***S* and **3***T*).

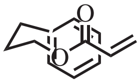

Stacking (*S*)

3*S*

Standard orientation: opt MPWB95/6–311++g(2d,2p) 6d iop(3/76=0690003100)
E = −616.04311982 a.u.

Center Number	Atomic Number	Atomic Type	Coordinates (Angstroms)		
			X	Y	Z
1	6	0	−2.609503	−0.405898	−0.299849
2	6	0	−2.009479	−1.789759	−0.232784
3	6	0	−0.862739	−1.946122	0.758964
4	6	0	−1.106478	1.396528	−0.012543
5	6	0	−0.126584	2.233052	−0.727717
6	8	0	−1.358837	1.470921	1.160490
7	6	0	0.581035	3.135353	−0.071208
8	6	0	0.456107	−1.333726	0.368475
9	6	0	0.988534	−1.475937	−0.906323
10	6	0	2.219681	−0.934492	−1.227611
11	6	0	2.947549	−0.242328	−0.276311
12	6	0	2.430956	−0.096562	0.997466
13	6	0	1.197545	−0.636920	1.311928
14	1	0	−2.912375	−0.057986	0.683009
15	1	0	−3.467736	−0.395475	−0.965527
16	1	0	−1.701191	−2.096138	−1.230878
17	1	0	−2.814236	−2.465274	0.057256
18	1	0	−0.705140	−3.012612	0.926260
19	1	0	−1.166187	−1.529154	1.718700
20	1	0	−0.013561	2.059479	−1.785685
21	1	0	1.312288	3.751685	−0.568765
22	1	0	0.435541	3.263562	0.990664
23	1	0	0.437702	−2.013711	−1.663359
24	1	0	2.612383	−1.056223	−2.225615
25	1	0	3.907607	0.180851	−0.527767
26	1	0	2.984908	0.445660	1.748303
27	1	0	0.788587	−0.498199	2.301736
28	8	0	−1.683455	0.529630	−0.854647

Table S8. Cartesian coordinates and energies of MPW1B95/6–311++G(2d,2p) geometry optimized structures 2 and 3 (conformations **2***S*, **2***T*, **3***S* and **3***T*).

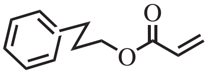

Trans (*T*)

3*T*

Standard orientation: opt MPWB95/6–311++g(2d,2p) 6d iop(3/76=0690003100)
E = −616.04509962 a.u.

Center Number	Atomic Number	Atomic Type	Coordinates (Angstroms)		
			X	Y	Z
1	6	0	1.378431	−0.519547	−0.439116
2	6	0	0.021948	0.050079	−0.124766
3	6	0	−1.090115	−0.836749	−0.671428
4	6	0	3.627879	−0.063060	−0.019085
5	6	0	4.568974	0.903826	0.577835
6	8	0	3.933895	−1.096864	−0.549874
7	6	0	5.867413	0.656882	0.574700
8	6	0	−2.454908	−0.352406	−0.283084
9	6	0	−3.128323	−0.931211	0.782341
10	6	0	−4.372039	−0.470619	1.175088
11	6	0	−4.965169	0.580915	0.502012
12	6	0	−4.306147	1.165137	−0.565624
13	6	0	−3.062363	0.701394	−0.952646
14	1	0	1.544481	−0.612023	−1.510983
15	1	0	1.510061	−1.508845	−0.005227
16	1	0	−0.062110	1.052256	−0.541922
17	1	0	−0.085401	0.148595	0.954170
18	1	0	−0.953501	−1.851305	−0.298211
19	1	0	−1.011081	−0.891196	−1.757128
20	1	0	4.147038	1.798497	1.007510
21	1	0	6.575370	1.346313	1.005589
22	1	0	6.239944	−0.255135	0.133099
23	1	0	−2.672705	−1.756484	1.310448
24	1	0	−4.879407	−0.935899	2.006084
25	1	0	−5.936618	0.941377	0.802291
26	1	0	−4.763916	1.981861	−1.102385
27	1	0	−2.557465	1.159364	−1.791532
28	8	0	2.365083	0.356211	0.106228

Table S9. Cartesian coordinates and energies of MPW1B95/6–311++G(2d,2p) geometry optimized structures 2 and 3 (conformations **2***S*, **2***T*, **3***S* and **3***T*).

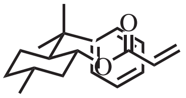

Stacking (*S*)

2*S*

Standard orientation: opt MPWB95/6–311++g(2d,2p) 6d
iop(3/76=0690003100)
E = – 889.95725590 a.u.

Center Number	Atomic Number	Atomic Type	Coordinates (Angstroms)		
			X	Y	Z
1	6	0	2.331005	–1.627212	0.455650
2	6	0	3.507622	–1.130442	–0.366033
3	6	0	3.653796	0.378438	–0.308342
4	6	0	2.343372	1.014901	–0.735864
5	6	0	1.189533	0.522705	0.108701
6	6	0	1.010548	–0.984163	0.034725
7	6	0	–0.218328	–1.500643	0.842150
8	6	0	–0.132532	–3.021380	1.019936
9	6	0	–0.238204	–0.878701	2.232940
10	6	0	–1.515384	–1.228604	0.086112
11	6	0	–1.690385	–1.733447	–1.198849
12	6	0	–2.867359	–1.543190	–1.895247
13	6	0	–3.913868	–0.845043	–1.317764
14	6	0	–3.761782	–0.346477	–0.039299
15	6	0	–2.577049	–0.537811	0.651888
16	6	0	4.811959	0.868937	–1.154230
17	8	0	–0.011678	1.149651	–0.358136
18	1	0	2.261577	–2.706405	0.357936
19	1	0	2.517015	–1.421030	1.512003
20	1	0	4.424885	–1.609965	–0.025842
21	1	0	3.370578	–1.426568	–1.409313
22	1	0	3.840484	0.659440	0.731871
23	1	0	2.398303	2.099639	–0.657332
24	1	0	2.144420	0.773277	–1.782194
25	1	0	1.351799	0.830703	1.138932
26	1	0	0.846639	–1.237400	–1.014861
27	1	0	–1.065259	–3.391368	1.437935
28	1	0	0.032505	–3.530182	0.072396
29	1	0	0.671270	–3.294853	1.698859
30	1	0	–1.011603	–1.337774	2.844414
31	1	0	–0.416427	0.193592	2.212433
32	1	0	0.713517	–1.047652	2.731845
33	1	0	–0.892623	–2.289475	–1.668868
34	1	0	–2.969550	–1.945180	–2.891741
35	1	0	–4.835826	–0.696858	–1.858107
36	1	0	–4.566671	0.199725	0.428417
37	1	0	–2.488863	–0.126661	1.643985
38	1	0	4.918019	1.949771	–1.093272
39	1	0	5.750612	0.420917	–0.835093
40	1	0	4.658769	0.608365	–2.200880
41	6	0	–0.460660	2.212812	0.312062
42	6	0	–1.690968	2.736291	–0.312544
43	8	0	0.067027	2.671449	1.292019
44	1	0	–2.069952	2.197855	–1.166271
45	1	0	–3.178163	4.215578	–0.264265
46	6	0	–2.279285	3.814588	0.175675
47	1	0	–1.860438	4.314354	1.035933

Table S10. Cartesian coordinates and energies of MPW1B95/6–311++G(2d,2p) geometry optimized structures 2 and 3 (conformations **2***S*, **2***T*, **3***S* and **3***T*).

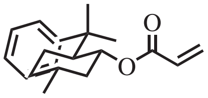

Trans (*T*)

2*T*

Standard orientation: opt MPWB95/6–311++g(2d,2p) 6d
iop(3/76=0690003100)
E = −889.95629860 a.u.

Center Number	Atomic Number	Atomic Type	Coordinates (Angstroms)		
			X	Y	Z
1	6	0	0.821841	1.591542	0.398574
2	6	0	0.205070	2.908760	–0.031916
3	6	0	–1.282062	2.963247	0.261273
4	6	0	–1.948187	1.760405	–0.380121
5	6	0	–1.318472	0.461235	0.074057
6	6	0	0.161885	0.379122	–0.262641
7	6	0	0.856243	–0.963863	0.133734
8	6	0	0.429509	–1.396728	1.530168
9	6	0	0.497517	–2.099024	–0.834413
10	6	0	2.364530	–0.767029	0.038666
11	6	0	3.204442	–0.821085	1.140957
12	6	0	4.571130	–0.629263	1.013264
13	6	0	5.128850	–0.375028	–0.223285
14	6	0	4.304665	–0.315095	–1.334140
15	6	0	2.944506	–0.510268	–1.200794
16	6	0	–1.910956	4.260598	–0.206043
17	8	0	–2.024237	–0.619795	–0.557264
18	1	0	1.882937	1.595474	0.172637
19	1	0	0.738811	1.492783	1.483582
20	1	0	0.716865	3.735352	0.459822
21	1	0	0.355207	3.044860	–1.106137
22	1	0	–1.414830	2.882377	1.343562
23	1	0	–3.009211	1.733772	–0.137528
24	1	0	–1.860748	1.831997	–1.466523
25	1	0	–1.454966	0.362341	1.148696
26	1	0	0.265505	0.489956	–1.345795
27	1	0	0.974094	–2.286609	1.836911
28	1	0	0.597187	–0.624719	2.278399
29	1	0	–0.629006	–1.644158	1.538751
30	1	0	1.156006	–2.947012	–0.659990
31	1	0	0.614726	–1.794619	–1.871350
32	1	0	–0.524794	–2.428098	–0.698504
33	1	0	2.798769	–1.011082	2.121180
34	1	0	5.198865	–0.678559	1.889876
35	1	0	6.192477	–0.225508	–0.323625
36	1	0	4.723789	–0.116873	–2.308800
37	1	0	2.320278	–0.456402	–2.080025
38	1	0	–2.973936	4.291895	0.022887
39	1	0	–1.439864	5.119335	0.267453
40	1	0	–1.799235	4.373568	–1.283932
41	6	0	–3.098297	–1.092146	0.081383
42	6	0	–3.729225	–2.179898	–0.692510
43	8	0	–3.485592	–0.688779	1.146166
44	1	0	–3.276335	–2.435603	–1.637432
45	1	0	–5.275618	–3.596385	–0.770898
46	6	0	–4.799854	–2.797937	–0.224725
47	1	0	–5.217154	–2.504755	0.726639

Table S11. Cartesian coordinates and energies of MPW1B95/6–311++G(2d,2p) geometry optimized structures 2 and 3 (conformations **2***S*, **2***T*, **3***S* and **3***T*).

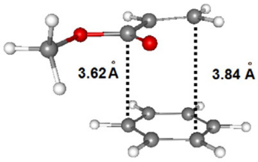

4

Standard orientation: opt MPWB95/6–311++g(2d,2p) 6d
iop(3/76=0690003100)
E = –538.63055147 a.u.

Center Number	Atomic Number	Atomic Type	Coordinates (Angstroms)		
			X	Y	Z
1	6	0	–3.051402	–1.352407	–0.011567
2	6	0	–1.711069	0.543924	–0.002474
3	6	0	–0.881434	1.435478	–0.830656
4	8	0	–1.912665	0.663865	1.176038
5	6	0	–0.309025	2.498546	–0.294047
6	8	0	–2.232194	–0.447186	–0.736330
7	1	0	–3.893472	–0.830604	0.432357
8	1	0	–3.392957	–2.086629	–0.729660
9	1	0	–2.481858	–1.828228	0.781063
10	1	0	–0.763621	1.170501	–1.868951
11	1	0	0.308695	3.162493	–0.876644
12	1	0	–0.450999	2.713996	0.754138
13	6	0	0.965065	–1.304899	0.799157
14	6	0	1.199605	–1.542082	–0.543669
15	6	0	2.129853	–0.779156	–1.228682
16	6	0	2.825814	0.217782	–0.569072
17	6	0	2.590012	0.454514	0.774096
18	6	0	1.655620	–0.303000	1.457294
19	1	0	0.235547	–1.893598	1.333474
20	1	0	0.656612	–2.320164	–1.057517
21	1	0	2.313812	–0.964411	–2.275780
22	1	0	3.554326	0.810019	–1.101253
23	1	0	3.132793	1.233051	1.287800
24	1	0	1.461752	–0.112047	2.501026

Table S12. Cartesian coordinates and energies of MPW1B95/6–311++G(2d,2p) geometry optimized structures to the complex **4**.

BENZENE

Standard orientation: opt MPWB95/6–311++g(2d,2p) 6d
iop(3/76=0690003100)
E = –232.19609986

Center Number	Atomic Number	Atomic Type	Coordinates (Angstroms)		
			X	Y	Z
1	6	0	–0.215622	1.366749	0.000000
2	6	0	–1.291600	0.496640	–0.000011
3	6	0	–1.076046	–0.870020	0.000011
4	6	0	0.215634	–1.366748	–0.000001
5	6	0	1.291596	–0.496651	–0.000010
6	6	0	1.076038	0.870030	0.000008
7	1	0	–0.384603	2.432500	0.000006
8	1	0	–2.299044	0.883216	–0.000010
9	1	0	–1.914544	–1.549198	0.000014
10	1	0	0.384583	–2.432503	0.000000
11	1	0	2.299051	–0.883197	–0.000003
12	1	0	1.914557	1.549182	0.000011

Table S13. Cartesian coordinates and energies of MPW1B95/6–311++G(2d,2p) geometry optimized structures to the complex 4.

METHYL ACRYLATE

Standard orientation: opt MPWB95/6–311++g(2d,2p) 6d
iop(3/76=0690003100)
E = – 306.43239576 a.u.

Center Number	Atomic Number	Atomic Type	Coordinates (Angstroms)		
			X	Y	Z
1	6	0	–0.040557	0.105756	–0.000047
2	6	0	–1.310024	–0.644225	–0.000044
3	1	0	–1.244640	–1.720576	–0.000118
4	6	0	–2.462937	0.001994	0.000059
5	1	0	–2.473278	1.081509	0.000132
6	1	0	–3.405133	–0.521743	0.000069
7	6	0	2.274613	–0.078066	0.000043
8	1	0	2.380204	0.545210	0.882364
9	1	0	3.012300	–0.869703	0.000133
10	1	0	2.380313	0.545106	–0.882339
11	8	0	1.008010	–0.724008	0.000001
12	8	0	0.064948	1.302438	–0.000040